Texas A&M
Coll. Station

(NASA-CR-175796) ALTIMETRY DATA AND THE ELASTIC STRESS TENSOR OF SUBDUCTION ZONES Final Report (Texas A&M Univ.) 23 p HC A02/MF A01 CSCL 04A

N85-27425

Unclas G3/46 21292

Final report on the research
supported by Grant #NAG5-94
RF 4340

Altimetry Data and the Elastic Stress Tensor of Subduction Zones

Michele Caputo
May 1985

The aim of the studies to be made for this project is to determine the stress field in the lithosphere caused by the distribution of density anomalies associated to the geoidal undulations observed by the GEOS-3 and SEASAT Earth satellites in the Tonga region.

Since the geoidal undulations do not determine uniquely the density-anomaly distribution causing the undulations, different models of the lithosphere have been generated with different assumptions on the density distribution and geometry, all generating a geoid profile almost identical to the observed one.

The first model used is that with the Airy isostatic hypothesis (Christian 1984), it consists of a crust (defined as a lower-density layer) of density 2.85 laying on a lithosphere of density 3.35. The models obtained with different compensation depths give residual shortwavelength anomalies of the order of several tens of mgal and several tens of meters geoidal undulations. This clearly indicates that in the Tonga region there is no isostasy of the Airy type because the observed geoid has very smooth undulation of about 25 m over a distance of 2000 km.

We also used the Pratt isostatic hypothesis in a model consisting of a crust of variable density laying on a lithosphere of higher density. This model gives smaller residual anomalies (Wainright 1983) but still shows that in the Tonga region there is no isostasy of the Pratt type because the observed geoidal undulation are much smaller and smoother than the residual undulations associated to the Pratt model of isostasy.

It is thus clear that the density anomalies needed to produce the observed geoid are not producing isostatic equilibrium at any depth, and therefore there is no hydrostatic equilibrium. The estimate of the consequent deviatoric stress is the aim of the research.

To compute it one must therefore compute models of the lithosphere which reproduce the geoidal undulations observed by GEOS-3 and SEASAT.

The first model (a) (Fig.1) was generated by assuming that the density of the crust is 2.85 (Carlson and Raskin 1984) and that of the lithosphere below it is 3.35 and taking into account the density (or thickness) variation with time of the oceanic lithosphere (McAdoo and Martin 1984). This model leads to an oceanic crust 24 km thick landward of the trench and 32 km thick landward of the trench.

In a second model (b) (Fig. 2) the density of the crust is assumed 2.85 and that of the lithosphere below 3.50; this model gives an average thickness of 18 km for the crust seaward of the trench and 28 km landward of the trench.

This raises serious questions on the meaning of the discontinuity surface in the velocities of the seismic wave found at the depth of 6 km below the ocean bottom (Shor et al. 1970, Turcotte and Shubert 1982) and assumed to define the thickness of the crust; it is clear now that a better definition of the term crust is needed in order to distinguish between the discontinuities of the different physical parameters.

In all cases examined the oceanic lithosphere (Fig. 3, 4) has been assumed to vary in density with time at a rate of about $0.2\ 10^{-3}$ gr/cm^3 Myears (rather than in thickness) and this low rate density variation together with the thinner crust landward of the trench and the thinner downgoing slab are responsible for the long wave length geoidal undulation observed by GEOS-3 and SEASAT.

In both cases (a) and (b) the computed models of the geoid deviates from the observed by less than 2 meters.

The density distribution of models (a) and (b) have then been used to determine the maximum shear stress (mms) field caused by their load on the layers below.

To estimate the stress field in a layered spherical Earth model we used the method of Caputo (1961); however the formulae of that paper would not allow for the body force associated to buoyant masses and had to be modified accordingly (Caputo 1984); the new formulae allow to compute the stress field in a layered sphere caused by the most general distribution of surface tractions and body forces.

The most recent results (Caputo et al. 1984) obtained using these formulae indicate that the mss caused by a mountain range and by its isostatic compensation, when this is exactly one below the range, is limited to the layer under the load including the layer containing the isostatic adjustment (Tables 1, 2); when the isostatic mass is displaced with respect to the load then the mss extends to a much greater depth (Tables 3, 4). In all cases the mss is at the most one third of the load. It is to be noted that when the isostatic mass is exactly below the load the mss reaches its maximum at the surface of separation between the top layer and that containing the isostatic mass and then it decreases linearly to almost zero within the latter layer (Fig. 6).

We then applied these results to the density anomaly models across the Tonga Trench obtaining a first estimate of the mss at several depths below the sea surface. To do this we computed, at depth of 9 km, 31 km, 59, 80 km, the pressure caused by the masses above the respective depth

for all the density models previously obtained for the Tonga region. In all cases we found that the most important features (Fig. 5) were pressure variations over relatively short horizontal distances which could be simulated by a box-like normal-traction (positive or negative) as considered by Caputo et al (1984) or a step like variation. The latter being the less relevant case in terms of the amount of traction variation.

The mss found in the Tonga region has several features. Maximum shear stress (mss) of about 300 bar are found close to the Trench (region A), and in the back area region (region B) extending to a great depth in the volume between them.

The analysis of the seismic activity in the Tonga region reveals that this is concentrated in regions A and B. In regions A and B there is normal depth seismic activity with moderate to large magnitudes, while between the two regions, as well known, the seismicity extends to a depth about 650 km.

It is important to note that there are other places in the Tonga region where the mss reaches values of 200 bar and there is no evidence of occurrence of large earthquakes in recent times namely in the area about 800 km landward of the trench. Detailed analysis of the seismicity of these regions may possibly reveal that they can be considered as locations of possible seismic gaps.

In this research it has also been found that the portion of the lithosphere under the seamount, in the cross section analysed, is not in isostatic equilibrium, and that the mss under the seamount is of the order of 250 bar at a depth below 50 km.

The stress field under seamounts had been estimated by Lambeck and Nakibogln (1980) and previously by other authors who modeled the deflection of the ocean lithosphere and gave values of more than 10 kbar for the mss (Walcott 1970, 1976, Watts et al. 1975); however Lambeck and Nakibogln (1980) argued that there are some plausible methods of reducing this mss and suggested that the mss should not exceed 1 kbar. The hypotheses invoked by Lambeck are lower density for the sediments fill in, depth-dependent nonelastic rheology and large-deflection, theory for the large loads.

The models determined in this research confirm that even without invoking the causes hypothesized by Lambeck and Nakibogln (1980) the mss under the seamount should always be about one third the load caused by the mount; which in the case of the seamounts studied by Lambeck would imply a mss less than 0.5 kbar.

It well known that rheology may set constraints on the mss that may have been accumulated in a region. It also known that there is no evidence that the Mantle and/or the Lithosphere may be described as Maxwell or Standard Linear Solids although several authors have tentatively used these models in their studies. In order to determine the effect of other possible rheologies we studied models different from the Maxwell and the Standard Linear Solid (Caputo 1984a); some of these models are supported by laboratory data (Caputo 1984b, Caputo 1984c).

Concerning the effect of rheology in the estimate of the mss of the lithosphere we must note that the theoretical research conducted in this project (Caputo 1984a) has shown that the relaxation time τ defined as the time to reduce the stress to e^{-1} of its initial value is not

indicative of the state of stress of a material at times $t >> \tau$, because there are rheological models which would maintain the e^{-1} reduced value of the initial stress for an almost indefinite time (Fig. 7, Caputo 1984a). Therefore the stress estimates computed in this research may have to be increased due to the residual stresses accumulated in previous time. It is also implied (Caputo, 1984d) that other phenomena such as the elastic rebound and their effect on the J_2 may have time history different from that assumed; for instance the variation of the J_2 may be due to the superposition of the effects of more than one glacial period.

The research made for this project concerning the rheological models of the mantle has also show that using the rheological models resulting from laboratory data on granite the response of the mantle to applied stress fields is such that relaxation times is almost independent of the wavelength of the stress field applied (Caputo, 1984b, Fig. 8).

A final note on the subduction zone process is due. Giardini and Woodhouse (1984) discussed 17 moment tensor solutions in the Tonga region and their implications for deformation within the subduction zone; they found a complex cross-cutting pattern of interacting shear bands and concluded that the Benioff zone should be seen "as that part of the convective flow which by virtue of temperature, composition and strain rate accomplishes its deformation through episodes of shear instability."

After the findings of this research, namely the theoretical estimates of the mss under mountain ranges (Caputo et al. 1984), the models of the lithosphere in the Tonga region and the mss distribution

underneath we may comment that the idea of the slab smoothly bending with very slowly varying density and or thickness defined by the seismicity distributions may need a revision but in a direction different than that of Giardini and Woodhouse (1984). One could view part of the seismicity as caused by the density anomalies distributions through the mss generated in the lithosphere and in the deeper layers, as the distribution of the latter is largely superimposed over the volume where the former occur.

Better evidence on this hypothesis could be supplemented by a detailed modelling of the mss under the Tonga region. This must now be obtained by computing it directly for the models of the density distribution of the lithosphere already determined rather than using the results of computations made for schematic models. More evidence should also be found by testing this hypothesis in other subduction regions of the world.

At this stage we have already obtained the density anomalies in two more profiles perpendicular to the Tonga Trench and we are in the process of computing the load at various depths due to these anomalies. From the load we shall infer the mss at depth.

The computer programme for the calculation of the mss in a layered spherical Earth has been completed to include the body forces in the two upper layers. This will allow to study more complex problem an obtain more realistic results.

The Research associated to the solution of the problems of this project led to the publication of the following papers:

Topography and its isostatic compensation as a cause of seismicity. Tectonophysics, 79, 73-83, 1983, Caputo M., Milana G., Rayhorn J.

Relaxation and free modes of a self-gravitating planet. Geophys. J. R. ast. Soc., 77, 789-808, 1984a. M. Caputo.

Topography and its isostatic compensation as a cause of seismicity, a revision, Tectonophysics, 111, 25-39, 1985a. Caputo M., Manzetti V., Nicelli R.

Spectral Rheology, Proceeding Symposium Space Techniques for Geodynamics, Hungarian Acad. of Sc., J. Somogi, C. Rigberg Ed., 1984b. M. Caputo.

Determination of the creep, fatigue and activation energy from constant strain rate experiment. Tectonophysics, 91, 157-164, 1983, M. Caputo.

Nonlinear and inverse rheology of rocks, 1985c. M. Caputo, (In press).

Generalized rheology and geophysical consequences, Tectonophysics, 1985d.

and to the following theses:

Wainright E.J., Calculation of isostatic gravity anomalies and geoid heights using two dimensional filtering: implications for structure in subduction zones, Ph.D. Dissertation, Graduate College of Texas A&M University, 1983.

Christian B.E., Utilization of satellite geoidal anomalies for computer analysis of Geophysical models. Master thesis, Graduate College of Texas A&M University, 1985.

Sevuklekin M.T., The estimate of the shear stress field of a self gravitating elastic planet during its formation. Master Thesis, Graduate College of Texas A&M University, 1984.

Martin Robert, The propagation of the stress due to the ridge push. (In progress).

Mecham Brent, The distribution of maximum shear stress is subduction zones due to topography and isostatic compensation. (In progress).

References

Caputo M., Deformation of a Layered Earth by an Axially Symmetric Surface Mass Distribution, J. Geophys. Res., 66, 1479-1483, 1961.

Caputo M., Relaxation and Free Modes of a Self-Gravitating Planet, Geophys. J. R. ast. Soc., 77, 789-808, 1984a.

Caputo M., Spectral Rheology, Proceeding Symposium Space Techniques for Geodynamics, Hungarian Acad. of Sc., J. Somogi, C. Reigberg Ed., 1984b.

Caputo M., Nonlinear and Inverse rheology of rocks, 1985e. (In press).

Caputo M., Topography and its Isostatic Compensation as a Cause of Seismicity, a Revision, Tectonophysics, 111, 25-39, 1985b.

Caputo M., Generalized rheology and geophysical consequences, Tectonophysics (In press), 1985c.

Carlson R.L. and Raskin G.S., Density of the ocean crusts, Nature, 311, 5986; 555-558, 1984.

Giardini F. and Woodhouse J.H., Deep Seismicity and Modes of Deformation in Tonga Subduction Zone, Nature, 307, 5951, 505-509, 1984.

Lambeck K. and Nakiboglu S.M., Seamount Loading and Stress in the Ocean Lithosphere, J. Geophys. Res. 85, B11, 6403-6418, 1980.

McAdoo D.C. and C. Martin, Seasat observations of Lithosphere Flexure Seaward of the Trenches, J. Geophys. Res. 89, 3201-3210, 1984.

Shor G.G., Menard H.W., Raitt R.W., Structure of the Pacific basin, in the Sea, A. Maxwell Ed., Wyley-Interscience, 3-28, 1970.

Walcott R., Flexure of the Lithosphere at Hawaii, Tectonophysics, 9, 435-446, 1970.

Walcott R., Lithospheric flexure, analysis of gravity anomalies and the propagation of seamount chains, The Geoph. of Pacific Ocean, Geoph. Mon. Ser. 19, eds. Sutton; Manghnani, Moberly, AGU, 1976.

Watts A.B., On Geoid Heights Derived from Geos-3 Altimeter Data Along the Hawaiian-Emperor Seamount Chain, J. Geophys. Res., 84, 3817-3876, 1979.

TABLE 1

Maximum shear stress in the spherically layered Earth model described in the text. The first and the second layers are 30 km thick. The load of 350 bar is applied to a strip of the outer surface defined by lat. 43.5° and 45°. The buoyant mass in the second layer is acting between the same latitudes. The contours are at 20 bar, 70 bar, 120 bar.

Latitude										Depth (km)	
42°		43°		44°		45°		46°			
11	16	11	65	111	111	65	11	17	11	5	0	1 st
11	18	11	66	113	114	66	11	18	11	6		layer
12	20	11	66	116	116	67	11	20	12	6		
12	21	11	67	115	114	67	11	21	12	6		
12	22	12	68	119	119	68	12	22	12	7		
12	23	13	68	120	121	68	13	23	13	7	15	
13	23	13	69	121	121	69	14	24	13	7		
13	14	14	69	122	122	76	15	24	13	7		
13	24	16	70	122	122	70	16	24	13	8		
12	24	17	70	122	122	70	17	24	13	8		
12	24	19	71	121	122	71	19	24	12	8	30	
12	24	19	71	121	122	71	19	24	12	8	30	2 nd
11	22	20	65	110	111	65	20	23	11	7		layer
10	21	21	60	99	99	60	21	21	10	6		
9	19	22	54	87	87	54	22	19	9	6		
8	17	23	49	75	75	49	23	17	8	5		
7	15	24	44	63	63	44	24	15	7	4	45	
5	13	24	39	51	51	39	24	13	5	3		
4	12	25	35	39	39	55	25	12	4	3		
3	11	25	31	27	27	31	25	11	3	2		
1	11	25	25	17	17	24	25	11	1	2		
1	11	25	27	12	12	27	25	11	1	2	60	
9	17	25	31	35	35	31	25	17	10	3	60	3 rd
8	15	21	26	29	29	26	21	15	9	1		layer
6	13	18	22	25	25	22	18	13	8	4	70	
8	12	16	19	21	21	19	16	12	8	4		
8	11	14	16	17	17	16	13	11	8	5	80	
8	10	12	13	15	15	13	12	10	8	5		
8	9	11	11	13	13	11	10	9	8	6	90	
8	9	10	9	12	11	9	9	9	8	6		
8	9	9	8	10	10	8	9	9	8	6	100	
8	9	9	7	9	9	7	8	9	8	6		
8	9	8	6	8	8	6	8	9	8	6	110	

TABLE 2

As in Table 1 with the second layer 80 km thick, symmetric case.

Latitude											Depth (km)	
42°			43°		44°		45°		46°			
10	13	16	60	107	107	66	16	13	11	4	0	1st layer
11	14	14	67	111	111	67	14	14	11	5		
12	16	13	66	114	114	68	12	17	12	5		
13	18	12	69	117	118	69	12	19	13	5		
13	20	12	70	120	120	70	13	21	14	5		
14	22	13	71	123	123	71	13	22	14	5	15	
15	23	13	72	15	125	72	14	24	15	6		
15	24	14	73	126	126	73	15	25	15	6		
15	25	15	74	128	128	74	16	26	16	6		
16	26	17	74	129	129	74	17	26	16	6		
16	26	15	75	130	130	75	18	27	16	6	30	
	27	18	75	130	130	75	18	27	16	6	30	2nd layer
15	26	20	70	121	121	70	20	27	16	5		
14	25	22	65	110	110	65	22	25	14	4		
13	23	23	59	97	97	59	23	23	13	3		
11	21	23	53	84	84	53	23	21	11	2		
10	19	23	56	70	70	46	24	19	10	1	70	
9	17	23	39	55	55	39	23	17	8	1		
8	15	23	33	40	40	33	23	15	7	2		
7	15	23	26	26	26	26	23	15	7	3		
7	15	22	21	12	12	21	22	15	7	3		
9	16	21	16	10	10	18	21	16	8	4	110	
11	16	21	25	27	27	24	21	16	11	7	110	3rd layer
11	13	12	8	9	8	8	11	12	11	9		
9	10	10	9	8	8	8	10	10	9	6		
6	7	8	8	7	7	7	7	7	6	5		
5	6	6	6	6	6	6	6	5	5	4	310	
4	4	4	4	4	6	4	4	4	4	3		
3	3	3	3	3	3	3	3	3	3	3		
3	3	3	3	3	3	3	3	2	2	2		
2	2	2	2	2	2	2	2	2	2	2	510	
2	2	2	2	2	2	2	2	2	2	1		
1	1	1	1	1	1	1	1	1	1	1		

68

69

TABLE 3

Maximum shear stress in the spherically layered Earth model described in the text. The first and second layers are 30 km thick. The load of 350 bar is applied to a strip of the outer surface defined by the lat. 43.5° and 45°. The buoyant mass in the second layer is acting between the latitudes 42.75° and 44.75°. The contours are at 20 bar, 70 bar, 120 bar.

Latitude											Depth (km)	
42			43		44		45		46			
6	17	6	60	105	106	75	29	6	10	6	0	1 st layer
6	18	7	61	107	109	74	26	7	9	5		
7	20	9	62	108	112	73	23	8	9	4		
8	22	12	63	109	114	72	20	8	9	4		
9	23	16	63	112	116	72	18	10	9	3		
10	26	19	64	115	118	72	16	11	9	3	15	
11	25	22	65	117	120	72	16	12	9	3		
12	29	24	66	119	121	72	15	12	9	3		
12	30	27	68	120	122	72	15	13	9	3		
13	30	29	70	121	122	72	16	13	9	3		
13	31	31	71	121	122	73	16	13	9	3	30	
13	31	31	71	121	122	73	16	13	9	3	30	2 nd layer
14	31	33	73	116	113	69	15	16	8	5		
14	31	35	15	114	105	55	19	19	8	6		
15	31	37	76	110	96	49	25	22	9	8		
15	30	40	78	105	87	85	32	24	9	9		
16	29	42	79	104	79	44	35	27	10	10	15	
16	28	45	79	94	71	47	46	30	11	11		
16	28	48	80	85	65	32	52	33	12	12		
17	28	51	80	82	30	39	59	35	14	13		
17	28	55	80	75	57	67	65	36	15	13		
17	28	59	80	67	58	75	71	41	17	13	60	
23	40	58	72	72	69	66	66	38	18	14	60	3 rd layer
23	45	67	86	97	99	92	77	58	36	22		
17	39	62	70	80	83	78	66	51	34	18	160	
17	28	41	52	60	62	59	51	40	28	16		
17	24	32	38	44	46	44	39	31	23	16	260	
16	20	26	30	33	34	33	30	25	19	14		
14	17	21	24	26	26	26	23	20	16	13		
12	15	17	19	20	21	20	19	16	14	12		
11	12	14	16	16	17	16	15	15	12	10		
10	11	12	13	14	14	13	13	12	10	9		
9	10	10	11	11	11	11	11	10	9	8	560	

Top layer:

$\lambda = 3.8 \cdot 10^{11}$, $\mu = 3.8 \cdot 10^{11}$, $r_3 = 6.371 \cdot 10^8$, $r_2 = 6.341 \cdot 10^8$

Second layer:

$\lambda = 7.5 \cdot 10^{11}$, $\mu = 6.4 \cdot 10^{11}$, $r_1 = \textit{variable}$, $r_2 = 6.341 \cdot 10^8$

Core;

$\lambda = 6 \cdot 10^{12}$, $\mu = 6 \cdot 10^{12}$, $r_1 =$ variable, $r_0 = 0$

TABLE 4

As in Table 3 with the second layer 80 km thick, $\overset{non}{\lambda}$ symmetric case.

Latitude											Depth (km)	
42			43		44		45		46			
5	1	10	57	100	101	87	46	10	15	13	0	1 st layer
6	15	9	58	102	104	85	43	9	14	11		
7	16	12	60	104	106	84	38	9	14	10		
9	17	16	61	105	113	83	33	9	14	8		
12	19	20	62	106	116	82	29	11	14	7		
14	21	24	63	106	120	82	26	13	14	6	15	
15	24	27	64	113	123	82	23	15	15	6		
17	26	30	67	116	126	82	21	14	15	5		
18	28	33	70	120	128	82	19	16	15	4		
16	30	36	72	122	130	82	18	19	16	4		
19	31	38	74	125	131	83	17	20	16	4	30	
19	32	38	74	125	132	83	17	20	16	4	30	2 nd layer
20	25	42	60	126	126	74	12	24	15	4		
21	36	45	84	125	114	65	16	27	15	6		
20	37	47	86	122	110	58	27	30	14	7		
20	37	48	87	118	101	54	35	32	13	9		
19	36	50	87	111	91	52	43	32	11	10	80	
18	35	51	86	104	82	53	49	35	13	11		
17	34	53	83	94	73	57	55	36	14	12		
15	34	56	80	83	66	63	59	37	15	11		
12	34	60	75	71	66	70	61	37	18	10		
9	36	66	69	57	71	78	60	39	21	8	110	
23	43	62	76	83	80	69	58	36	21	12	110	3 rd layer
21	40	60	75	84	85	77	64	47	30	16		
19	33	47	60	67	69	64	54	41	27	15		
19	27	37	45	51	52	49	42	33	23	15		
16	23	29	35	36	39	37	37	26	20	14	310	
16	20	24	27	29	30	28	25	21	17	13		
14	17	19	22	23	23	22	20	18	15	12		
12	14	16	18	18	18	18	16	15	12	10		
11	12	14	14	15	15	15	14	12	11	9	510	
10	11	11	12	12	12	12	11	10	9	6		
9	9	10	10	11	11	10	10	9	8	7		

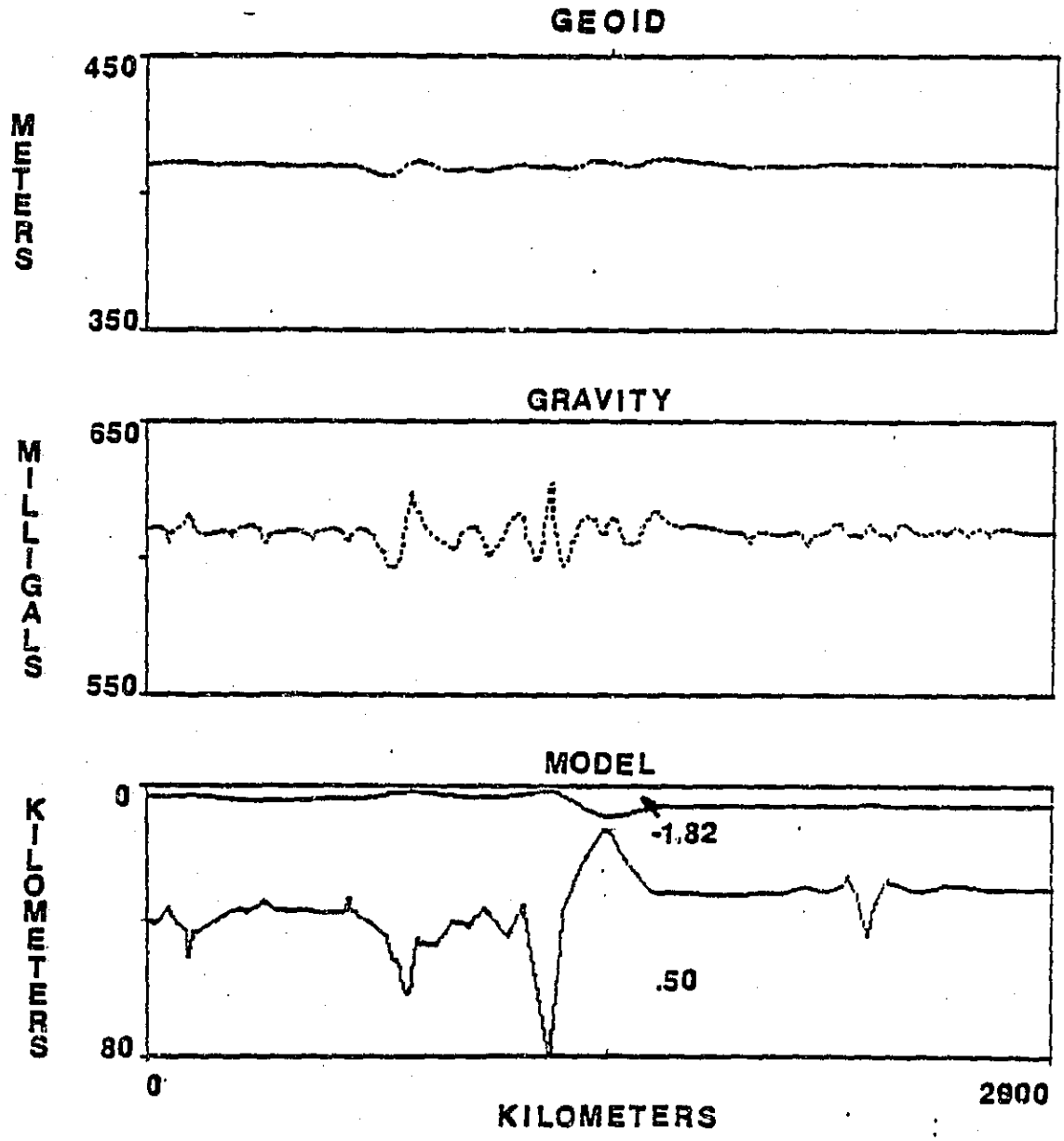

Figure 1 . Non-Isostatic model, seawater density 1.03, crust density 2.85, root density 3.35.

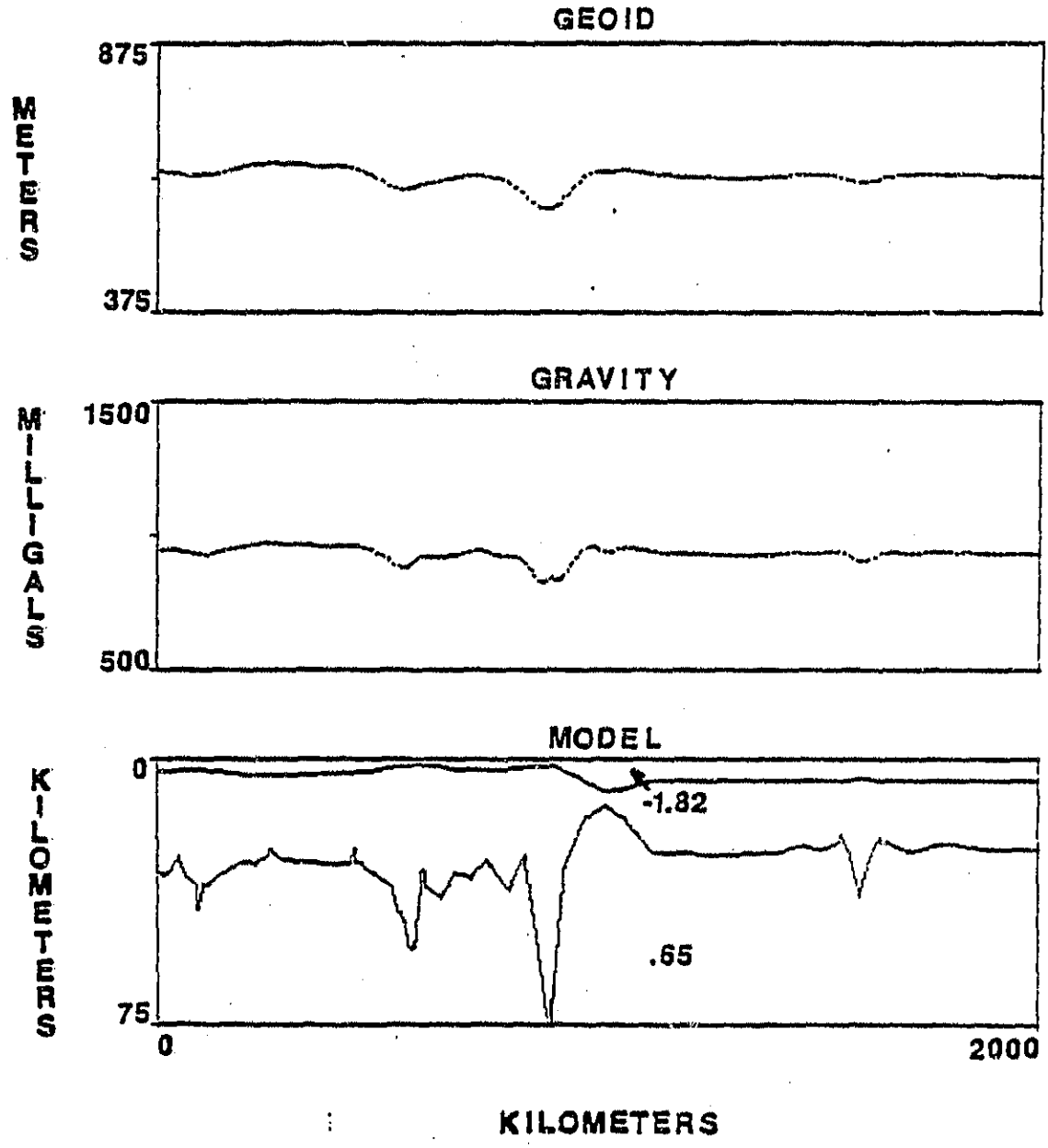

Figure 2. Non-Isostatic model, seawater density 1.03, crust density 2.85, root density 3.50.

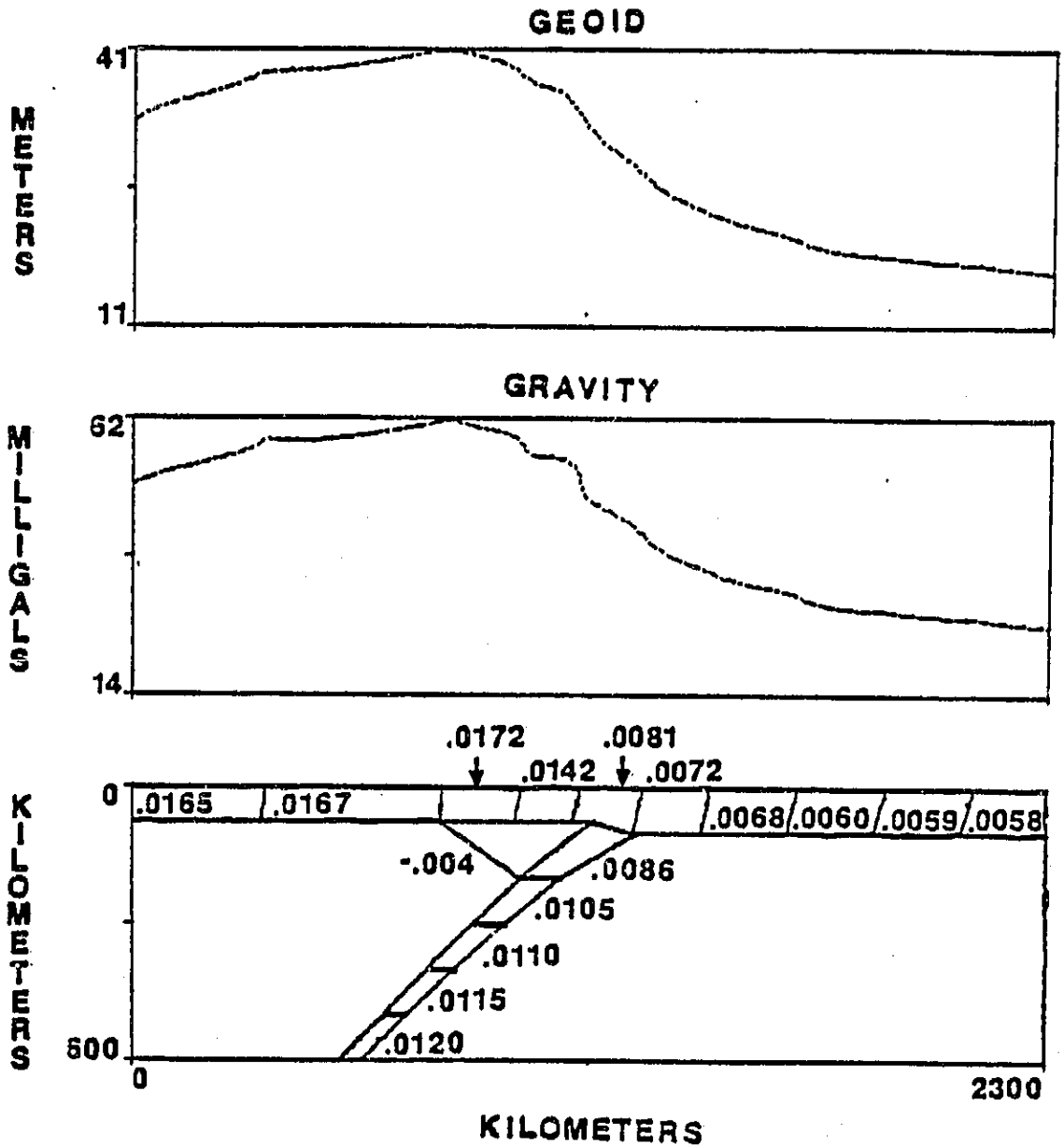

Figure 3 . Complete Slab-Lithosphere model, gravity and geoid profiles.

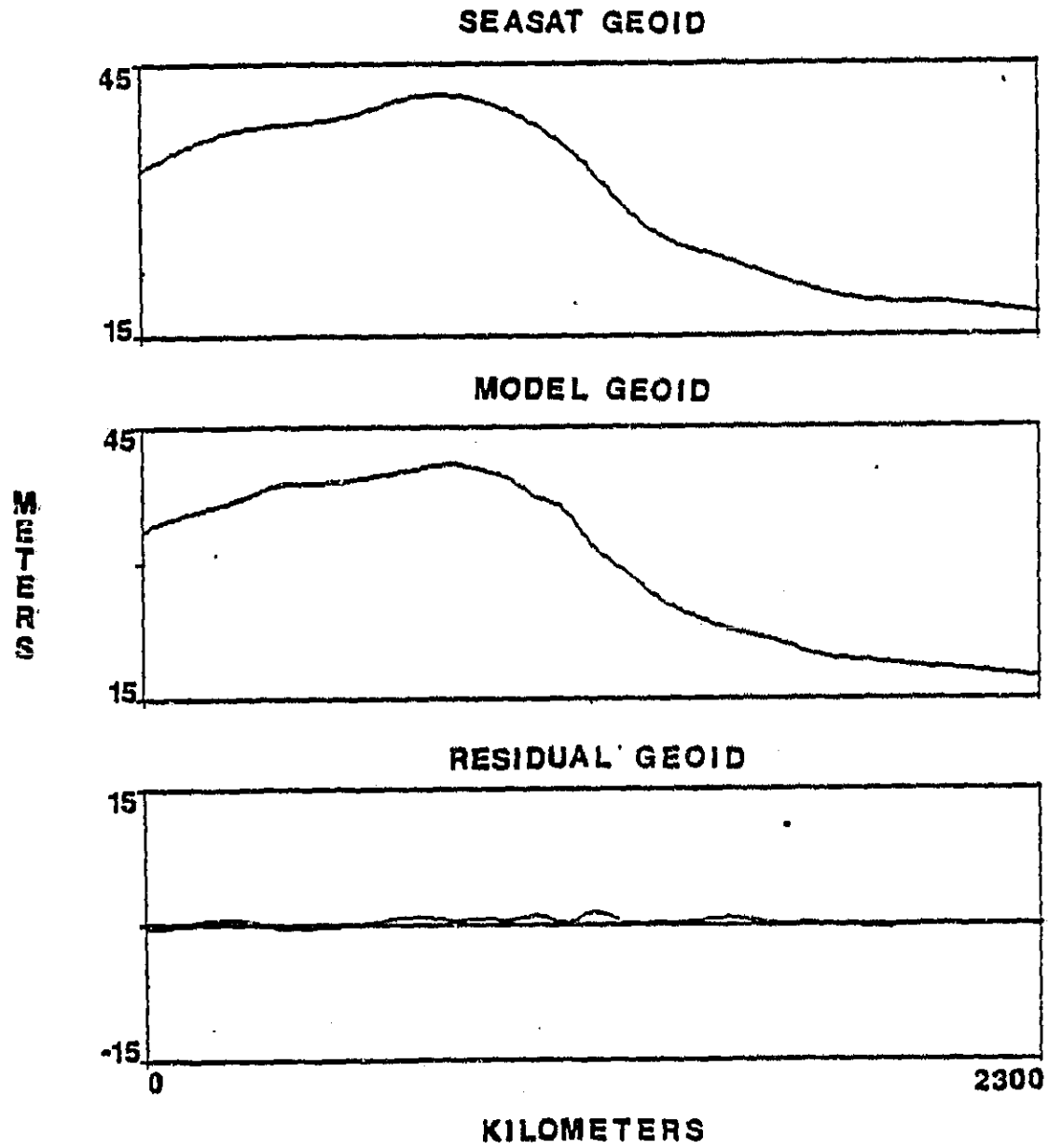

Figure 4. Complete Slab-Lithosphere model, Seasat, geoid and residual geoid.

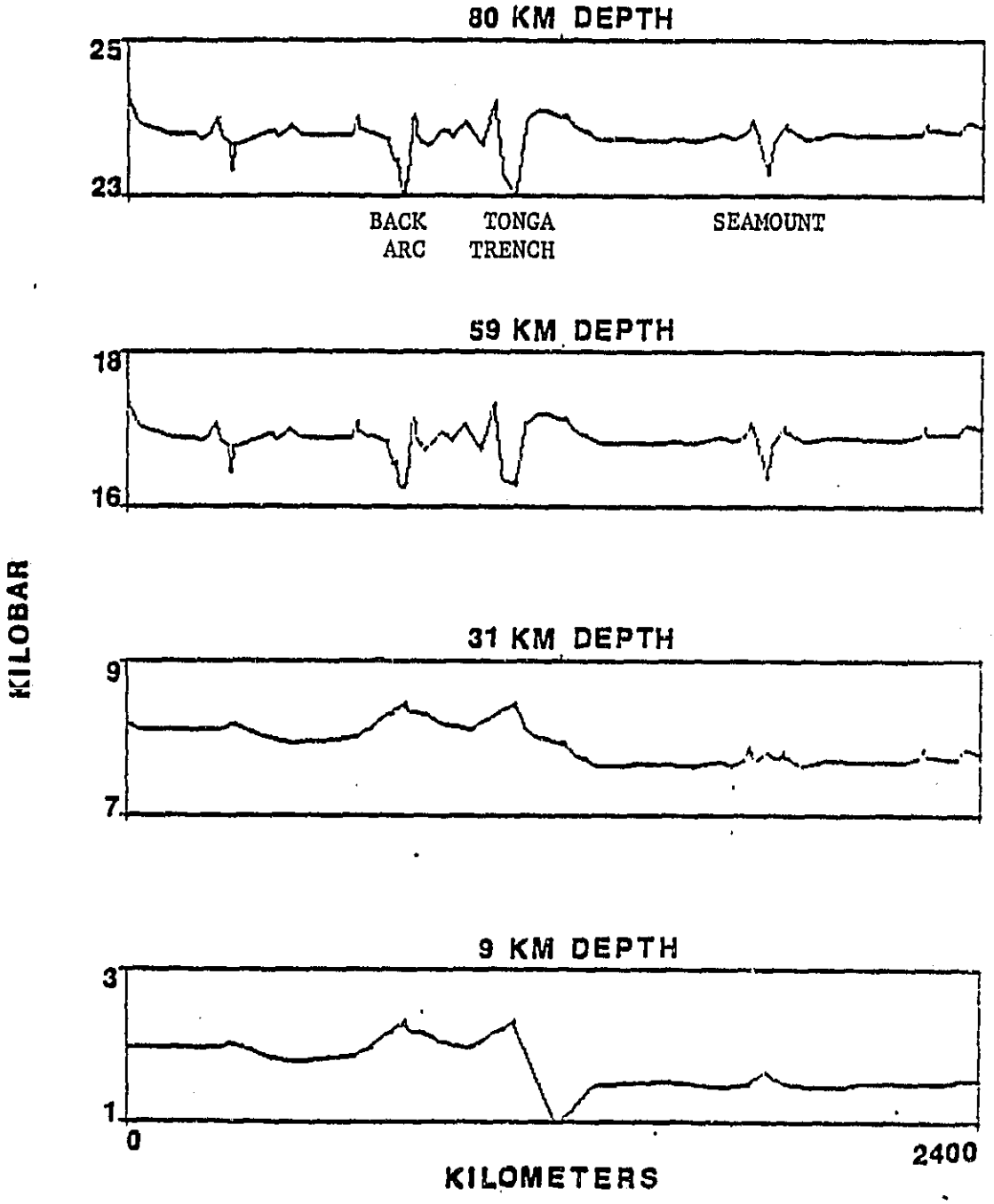

Figure 5. Pressure at depths of 9, 31, 59, and 80 kilometers.

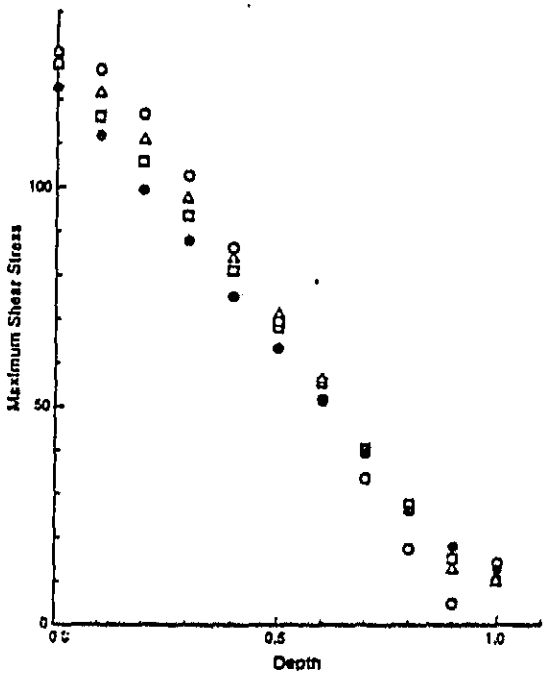

Fig 6 Maximum shear stress as function of depth in the second layer of the model (beginning at 30 km depth) given in Fig. 1. In each of the four cases considered for the thickness of the second layer, the depth measured from the top of the second layer is normalized to the thickness of the layer. Full circles refer to a second layer with 30 km thickness, squares refer to 55 km thickness, triangles refer to 80 km thickness, and open circles refer to 175 km thickness. Mss in bar.

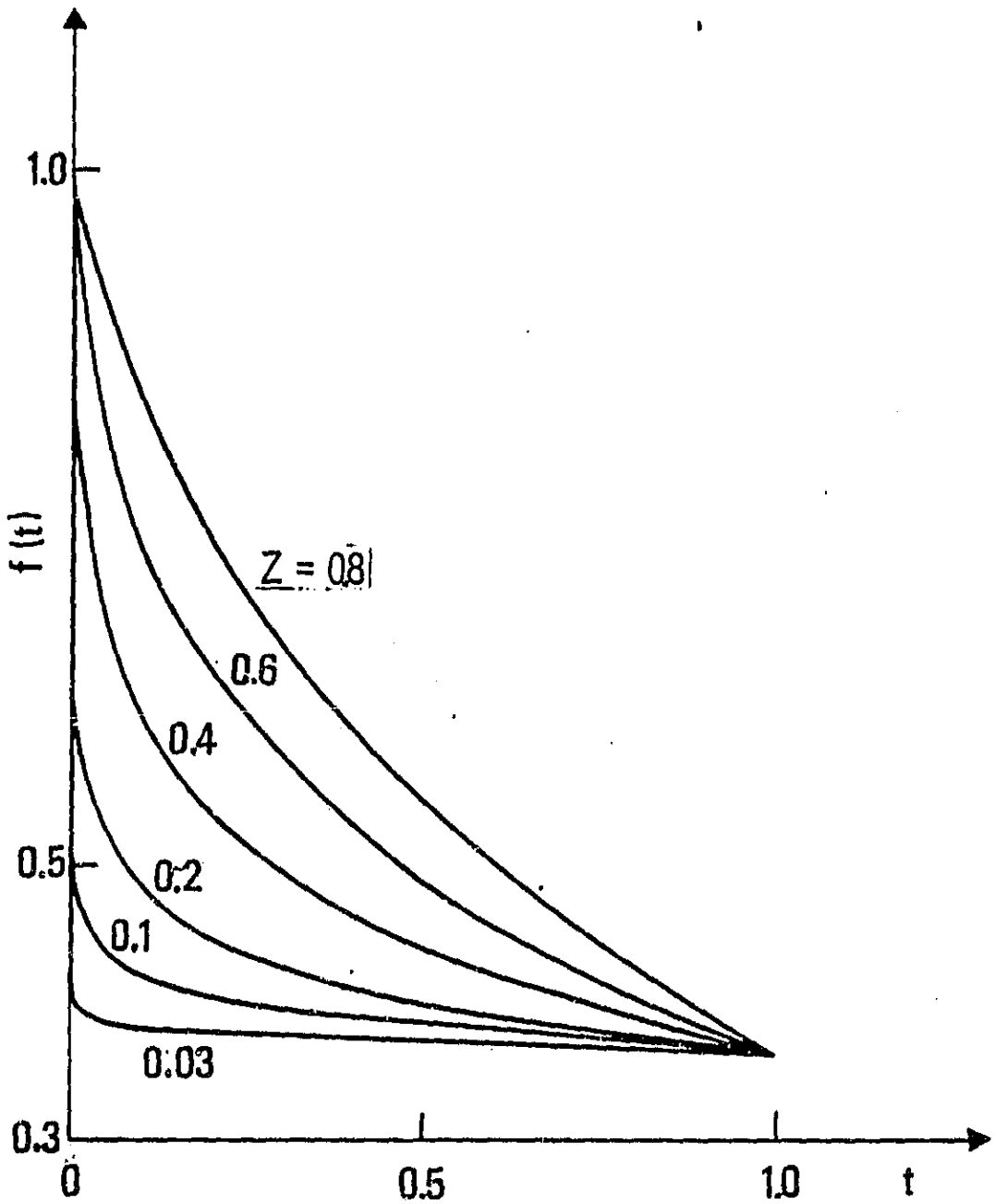

Figure 7. Relaxation time f(t) of the rheological models identified by the parameter Z; the relaxation time is assumed unit and is arbitrary; here f(t) is the same for all Z, only the time history of the relaxation depends on Z.

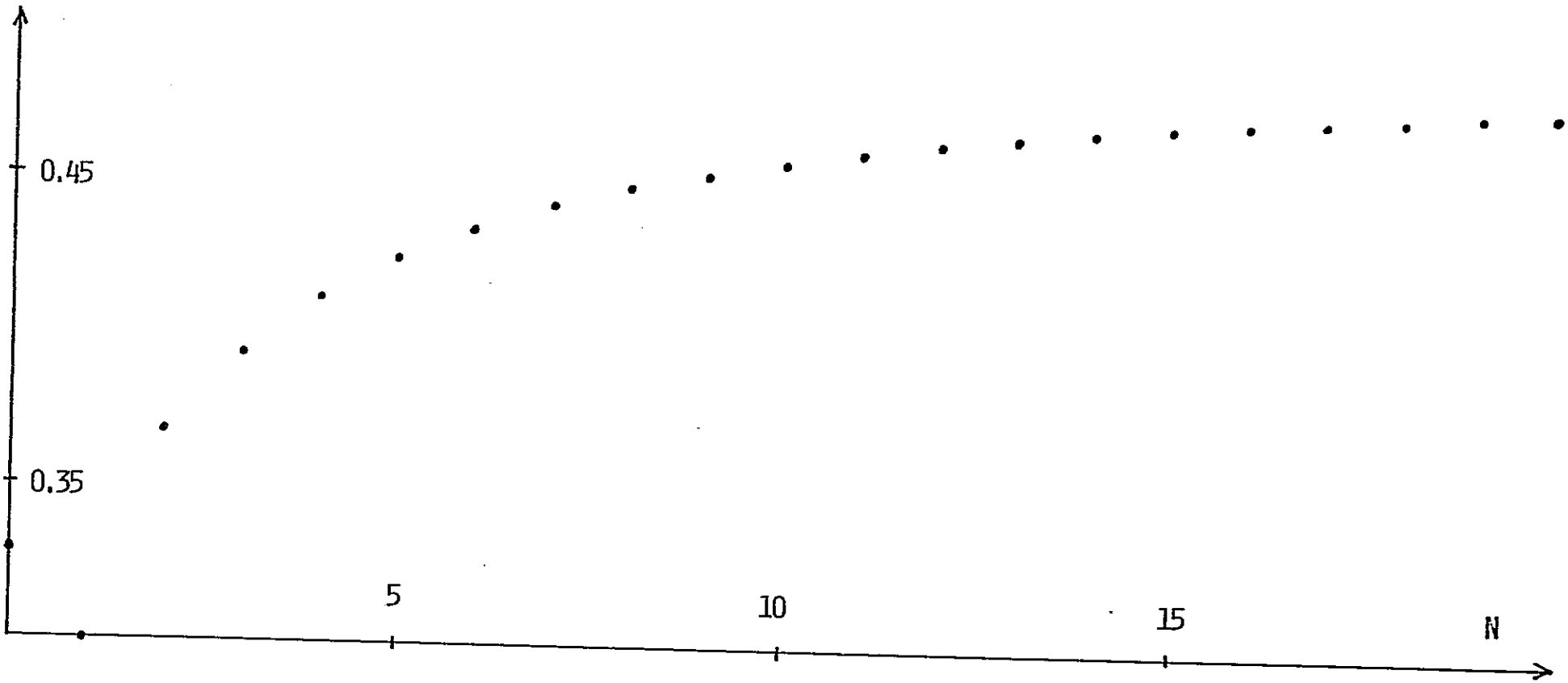

Figure 8. The relaxation time of a sphere with the rheology of granite determined from laboratory data is almost wave number independent. The stress described by a Legendre polinomial of order N has a relaxation time depending on junction of N given in the Figure. The asymptotic value for $N = \infty$ is 0.5.